Table 1. Baseline characteristics.

Variables	SR n = 5361	RFA n = 5548	PEI n = 2059	*p* value
Age, median (5, 95 percentile), yr	66 (48, 77)	69 (52, 80)	69 (52, 80)	<0.0001[a]
Sex				<0.0001[b]
Male, No. (%)	3967 (74.0)	3569 (64.3)	1303 (63.3)	
Female, No. (%)	1394 (26.0)	1979 (35.7)	756 (36.7)	
Hepatitis virus infection				<0.0001[b]
HBs Ag(+)/HCV-Ab(-), No. (%)	908 (16.9)	462 (8.3)	141 (6.8)	
HBs Ag(-)/HCV-Ab(+), No. (%)	3393 (63.3)	4263 (76.8)	1632 (79.3)	
HBs Ag(+)/HCV-Ab(+), No. (%)	106 (2.0)	87 (1.6)	32 (1.6)	
HBs Ag(-)/HCV-Ab(-), No. (%)	760 (14.2)	512 (9.2)	160 (7.8)	
Unknown	194 (3.6)	224 (4.0)	94 (4.6)	
Liver damage				<0.0001[b]
A, No. (%)	4000 (74.6)	3349 (60.4)	1204 (58.5)	
B, No. (%)	1361 (25.4)	2199 (39.6)	855 (41.5)	
Serum albumin, median (5, 95 percentile), g/dl	3.9 (3.1, 4.6)	3.7 (2.9, 4.4)	3.7 (2.8, 4.4)	<0.0001[a]
Serum total bilirubin, median (5, 95 percentile), mg/dl	0.8 (0.4, 1.5)	0.9 (0.4, 1.9)	0.9 (0.4, 2.2)	<0.0001[a]
Platelet count, median (5, 95 percentile), x 10^4/μl	12.6 (5.8, 24.0)	9.9 (4.5, 20.4)	9.5 (4.4, 19.6)	<0.0001[a]
ICG R15, median (5, 95 percentile), %	15 (5, 35)	22 (7, 51)	24 (8, 51)	<0.0001[a]
Tumor number				<0.0001[c]
Single, No. (%)	4458 (83.2)	4068 (73.3)	1449 (70.4)	
Two, No. (%)	706 (13.2)	1096 (19.8)	443 (21.5)	
Three, No. (%)	197 (3.7)	384 (6.9)	167 (8.1)	
Tumor size, median (5, 95 percentile), mm	23 (12, 30)	20 (10, 30)	17 (10, 30)	<0.0001[a]
Alpha-fetoprotein				<0.0001[b]
≥15 ng/ml, No. (%)	2726 (50.9)	3028 (54.6)	1125 (54.6)	
<15 ng/ml, No. (%)	2457 (45.8)	2301 (41.5)	828 (40.2)	
Unknown, No. (%)	178 (3.3)	219 (3.9)	106 (5.2)	
Des-γ-carboxy prothrombin				<0.0001[b]
≥40 AU/ml, No. (%)	2182 (40.7)	1593 (28.7)	541 (26.3)	
<40 AU/ml, No. (%)	2651 (49.5)	3322 (59.9)	1169 (56.8)	
Unknown, No. (%)	528 (9.9)	633 (11.4)	349 (17.0)	

HBsAg, hepatitis B virus antigen; HCV-Ab, hepatitis C virus antibody; ICG R15, indocyanine green retention rate at 15 min.
[a]ANOVA.
[b]Chi-square.
[c]Mante-trend test.

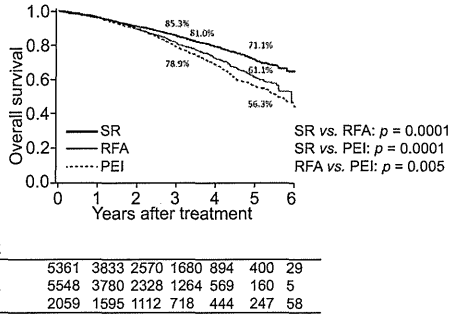

Patients at risk

SR	5361	3833	2570	1680	894	400	29
RFA	5548	3780	2328	1264	569	160	5
PEI	2059	1595	1112	718	444	247	58

Fig. 1. Overall survival curves after surgical resection (SR), radiofrequency ablation (RFA), and percutaneous ethanol injection (PEI).

into 8 subgroups according to 3 factors (liver damage class, tumor size, and number of tumors), which have repeatedly been shown to be clinically relevant prognostic factors. The results of the subgroup analyses indicated that surgical resection would effectively prevent recurrence in patients with relatively advanced HCC (2–3 cm in diameter) among the study populations, irrespective of liver damage class or number of tumors. This finding suggests that surgery might be superior to percutaneous ablation therapies in patients with a more advanced tumor stage. As for the subgroups with a single tumor, surgical resection yielded better overall survival and time to recurrence rates than RFA or PEI. Especially in the subgroup with a single tumor smaller than 2 cm in diameter, both the overall and time to recurrence rates were statistically significantly better after surgery than after RFA, whereas no such statistically significant differences in these two parameters between the two treatment groups were detected in a few subgroups with a single tumor, maybe due to the insufficient sample size of the subgroups. Thus, surgical resection would be considered as the treatment modality of first choice for a single HCC, as recommended by the Japanese clinical practice guideline [2]. Overall, there was a trend toward superior

Please cite this article in press as: Hasegawa K et al. Comparison of resection and ablation for hepatocellular carcinoma: A cohort study based on a Japanese nationwide survey. J Hepatol (2013), http://dx.doi.org/10.1016/j.jhep.2012.11.009

Research Article

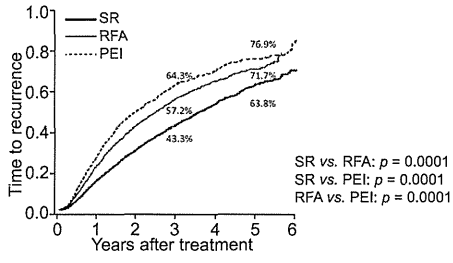

Patients at risk							
SR	5361	3265	1844	1039	451	189	15
RFA	5548	2954	1396	591	225	62	4
PEI	2059	1154	583	304	172	90	15

Fig. 2. Time to recurrence curves after surgical resection (SR), radiofrequency ablation (RFA), and percutaneous ethanol injection (PEI).

overall and time to recurrence rates after surgery than after RFA and PEI.

The reason why the long-term outcomes of the SR group were better than those of the PEI and RFA groups cannot be definitely clarified from the results of this study, however, in theory, surgical resection has the advantage of offering better local control of HCC over PEI and RFA, both of which have some potential risks of local recurrence associated with insufficient ablation. In addition, anatomic resection to remove minute tumor satellites [14] might have decreased the recurrence rate in the SR group, although this remains a speculation.

Recently, the latest trial from China [15], which had an adequate sample size (total 230 patients), reported that surgical resection yielded significantly better long-term outcomes than RFA. Although the study design was better than that of the two previously reported RCTs [10,11], it appeared to have limitations with respect to the results, such as drop in the overall survival in the RFA group as compared with that in the surgery group during the early period after treatment. The early deaths in the RFA group could have been treatment-related rather than cancer-related. Thus, no conclusion can be drawn from the three currently available RCTs.

One of the limitations of our study is the diversity of demographic factors in the study population, which would have been

Table 2. Hazard ratios for death and recurrence adjusted by multivariate analysis.

A For death

Variables		Hazard ratio	95% CI	*p* value
Treatments	SR *vs.* RFA	0.84	0.74, 0.95	0.006
	SR *vs.* PEI	0.75	0.64, 0.86	0.0001
	RFA *vs.* PEI	0.88	0.77, 1.01	0.08
Age	<65 *vs.* ≥65	0.71	0.63, 0.79	0.0001
Sex	Female *vs.* male	0.87	0.78, 0.98	0.03
HBsAg	Positive *vs.* negative	0.91	0.74, 1.11	0.34
HCV Ab	Positive *vs.* negative	0.93	0.79, 1.10	0.40
Liver damage	A *vs.* B	0.62	0.56, 0.69	0.0001
Platelet count	$\geq 10^4$ *vs.* $<10^4$/μl	0.76	0.68, 0.85	0.0001
Tumor size	<2 *vs.* ≥2 cm	0.82	0.73, 0.92	0.0007
Tumor number	Single *vs.* multiple	0.72	0.64, 0.80	0.0001
AFP	<15 *vs.* ≥15 ng/ml	0.66	0.59, 0.74	0.0001
DCP	<40 *vs.* ≥40 AU/ml	0.59	0.53, 0.66	0.0001

B For recurrence

Variables		Hazard ratio	95% CI	*p* value
Treatments	SR *vs.* RFA	0.74	0.68, 0.79	0.0001
	SR *vs.* PEI	0.59	0.54, 0.65	0.0001
	RFA *vs.* PEI	0.81	0.74, 0.88	0.0001
Age	<65 *vs.* ≥65	0.83	0.78, 0.89	0.0001
Sex	Female *vs.* male	0.88	0.82, 0.95	0.0001
HBsAg	Positive *vs.* negative	1.04	0.92, 1.17	0.53
HCV Ab	Positive *vs.* negative	1.15	1.04, 1.27	0.007
Liver damage	A *vs.* B	0.87	0.81, 0.93	0.0001
Platelet count	$\geq 10^4$ *vs.* $<10^4$/μl	0.92	0.86, 0.98	0.02
Tumor size	<2 *vs.* ≥2 cm	0.84	0.79, 0.90	0.0001
Tumor number	Single *vs.* multiple	0.69	0.64, 0.74	0.0001
AFP	<15 *vs.* ≥15 ng/ml	0.71	0.67, 0.76	0.0001
DCP	<40 *vs.* ≥40 AU/ml	0.72	0.67, 0.77	0.0001

HBsAg, hepatitis B virus surface antigen; HCV, hepatitis C virus; Ab, antibody; AFP, alpha-fetoprotein; DCP, des-γ-carboxy prothrombin; SR, surgical resection; RFA, radiofrequency ablation; PEI, percutaneous ethanol injection; CI, confidence interval.

Please cite this article in press as: Hasegawa K et al. Comparison of resection and ablation for hepatocellular carcinoma: A cohort study based on a Japanese nationwide survey. J Hepatol (2013), http://dx.doi.org/10.1016/j.jhep.2012.11.009

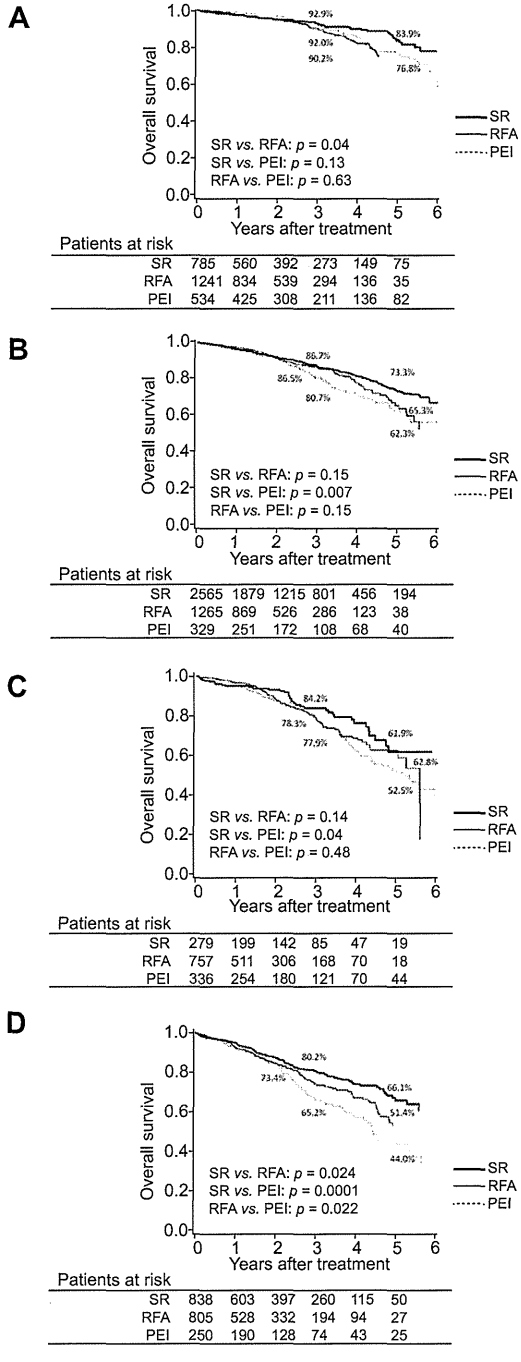

Fig. 3. Overall survival rates after surgical resection (SR), radiofrequency ablation (RFA), and percutaneous ethanol injection (PEI) in the subgroup of cases with single tumor and liver damage class A and B. (A) Liver damage class A, a single tumor (<2 cm); (B) liver damage class A, a single tumor (2–3 cm); (C) liver damage class B, a single tumor (<2 cm); (D) liver damage class B, a single tumor (2–3 cm).

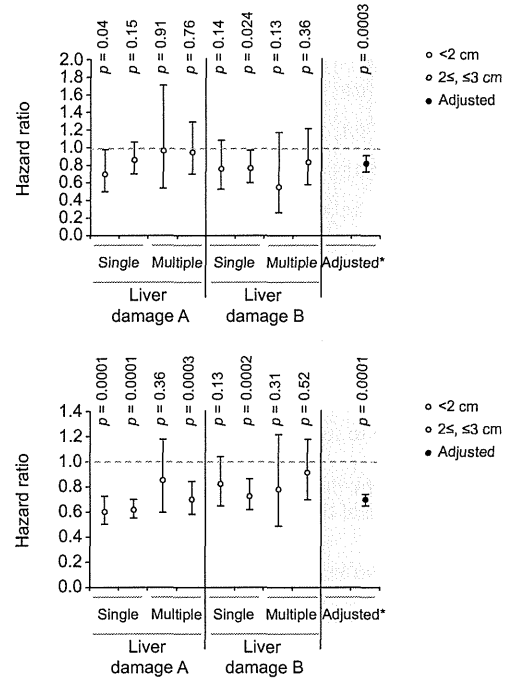

Fig. 4. Hazard ratios for death and recurrence with 95% confidence intervals and *p* values after surgical resection relative to those after radiofrequency ablation in the 8 subgroups. *The adjusted values for death and recurrence were calculated according to the three factors (tumor size, number of tumors, and liver damage class), as done in each subgroup. (A) Hazard ratios for death; (B) hazard ratios for recurrence.

caused by the selection process of treatment modalities. As similar to the previous retrospective studies [5–9], the patients amenable to surgery had had younger age, less prevalence of hepatitis C virus infection, better liver function, less association with portal hypertension, fewer number of tumors and lower alpha-fetoprotein level, whereas their tumor size was larger and their des-γ-carboxy prothrombin level was higher. To minimize potential effects of confounding factors, we studied patients who had similar tumor-related and liver function-related factors and performed multivariate analysis using 10 clinically important factors, similar to our previous study [9]. Although it is impossible to completely eliminate potential negative impacts of demographic diversity, we believe that our results are clinically meaningful, because of the large sample size of our study. In Japan, a nationwide RCT in patients with HCC is now ongoing, and the results are expected to lead to more definitive conclusions [16].

Another potential limitation of our study is the lack of data on liver function during the follow-up, which precluded assessment of the relationship between the liver function status and the choice of treatment at recurrence. In HCC, the influence of the first treatment is considered to be smaller than that in other primary malignant diseases, because the liver function remarkably affects the recurrence rate. Further investigations, particularly prospective clinical trials, are needed to address these issues.

In conclusion, this large cohort study based on data obtained by a nationwide survey in Japan, suggests that surgical resection may offer some advantage over RFA and PEI in terms of both overall survival and time to recurrence in patients with less advanced HCC. Although our results are considered as being more reliable than those of previous studies comparing the treatment

Please cite this article in press as: Hasegawa K et al. Comparison of resection and ablation for hepatocellular carcinoma: A cohort study based on a Japanese nationwide survey. J Hepatol (2013), http://dx.doi.org/10.1016/j.jhep.2012.11.009

Research Article

outcomes in HCC, our conclusions need to be confirmed by future RCTs.

Financial support

This study was supported by the Liver Cancer Study Group of Japan. There were no other sources of funding for any authors.

Conflicts of interest

The authors who have taken part in this study declared that they do not have anything to disclose regarding funding or conflict of interest with respect to this manuscript.

Acknowledgements

We all express our sincere thanks to Mr. Tomohiro Shinozaki, Ph.D. for his great contribution to the preparation of the data for statistical analyses.

References

[1] El-Serag HB. Hepatocellular carcinoma. N Engl J Med 2011;365:1118–1127.
[2] Makuuchi M, Kokudo N. Clinical practice guidelines for hepatocellular carcinoma: the first evidence based guidelines from Japan. World J Gastroenterol 2006;12:828–829.
[3] Bruix J, Sherman M, Llovet JM, Beaugrand M, Lencioni R, Burroughs AK, et al. Clinical management of hepatocellular carcinoma. Conclusions of the Barcelona-2000 EASL Conference. European association for the study of the liver. J Hepatol 2001;35:421–430.
[4] Bruix J, Sherman M. Management of hepatocellular carcinoma. Hepatology 2005;42:1208–1236.
[5] Montorsi M, Santambrogio R, Bianchi P, Donadon M, Moroni E, Spinelli A, et al. Survival and recurrences after hepatic resection or radiofrequency for hepatocellular carcinoma in cirrhotic patients: a multivariate analysis. J Gastrointest Surg 2005;9:62–67.
[6] Hong SN, Lee SY, Choi MS, Lee JH, Koh KC, Paik SW, et al. Comparing the outcomes of radiofrequency ablation and surgery in patients with a single small hepatocellular carcinoma and well-preserved hepatic function. J Clin Gastroenterol 2005;39:247–252.
[7] Guglielmi A, Ruzzenente A, Valdegamberi A, Pachera S, Campagnaro T, D'Onofrio M, et al. Radiofrequency ablation versus surgical resection for the treatment of hepatocellular carcinoma in cirrhosis. J Gastrointest Surg 2008;12:192–198.
[8] Arii S, Yamaoka Y, Futagawa S, Inoue K, Kobayashi K, Kojiro M, et al. Results of surgical and nonsurgical treatment for small-sized hepatocellular carcinomas: a retrospective and nationwide survey in Japan. The Liver Cancer Study Group of Japan. Hepatology 2000;32:1224–1229.
[9] Hasegawa K, Makuuchi M, Takayama T, Kokudo N, Arii S, Okazaki M, et al. Surgical resection vs. percutaneous ablation for hepatocellular carcinoma: a preliminary report of the Japanese nationwide survey. J Hepatol 2008;49:589–594.
[10] Huang GT, Lee PH, Tsang YM, Lai MY, Yang PM, Hu RH, et al. Percutaneous ethanol injection versus surgical resection for the treatment of small hepatocellular carcinoma: a prospective study. Ann Surg 2005;242:36–42.
[11] Chen MS, Li JQ, Zheng Y, Guo RP, Liang HH, Zhang YQ, et al. A prospective randomized trial comparing percutaneous local ablative therapy and partial hepatectomy for hepatocellular carcinoma. Ann Surg 2006;243:321–328.
[12] Hasegawa K, Kokudo N, Makuuchi M. Surgery or ablation for hepatocellular carcinoma. Ann Surg 2008;247:557–558.
[13] Ikai I, Arii S, Kojiro M, Ichida T, Makuuchi M, Matsuyama Y, et al. Reevaluation of prognostic factors for survival after liver resection in patients with hepatocellular carcinoma in a Japanese nationwide survey. Cancer 2004;101:796–802.
[14] Makuuchi M, Hasegawa H, Yamazaki S. Ultrasonically guided subsegmentectomy. Surg Gynecol Obstet 1986;161:346–350.
[15] Huang J, Yan L, Cheng Z, Du L, Wang J, Xu Y, et al. A randomized trial comparing radiofrequency ablation and surgical resection for HCC conforming to the Milan criteria. Ann Surg 2010;252:903–912.
[16] Hasegawa K, Kokudo N, Shiina S, Tateishi R, Makuuchi M. Surgery vs. radiofrequency ablation for small hepatocellular carcinoma: start of a randomized controlled trial (SURF trial). Hepatol Res 2010;40:851–852.

Please cite this article in press as: Hasegawa K et al. Comparison of resection and ablation for hepatocellular carcinoma: A cohort study based on a Japanese nationwide survey. J Hepatol (2013), http://dx.doi.org/10.1016/j.jhep.2012.11.009

EXPERIMENTAL CELL RESEARCH 319 (2013) 35–44

Available online at www.sciencedirect.com

SciVerse ScienceDirect

journal homepage: www.elsevier.com/locate/yexcr

Research Article

Involvement of hepatocellular carcinoma biomarker, cyclase-associated protein 2 in zebrafish body development and cancer progression

Kathryn Effendi[a], *Ken Yamazaki*[a], *Taisuke Mori*[a], *Yohei Masugi*[a], *Shinji Makino*[b], *Michiie Sakamoto*[a,*]

[a]*Department of Pathology, School of Medicine, Keio University, 35 Shinanomachi, Shinjuku-ku, Tokyo 160-8582, Japan*
[b]*Department of Regenerative Medicine and Advanced Cardiac Therapeutics, Center for Integrated Medical Research, School of Medicine, Keio University, Tokyo, Japan*

ARTICLE INFORMATION

Article Chronology:
Received 20 April 2012
Received in revised form
20 August 2012
Accepted 10 September 2012
Available online 27 September 2012

Keywords:
Skeletal muscle
Actin
Cancer
Development
HCC cells
Zebrafish

ABSTRACT

Cyclase-associated protein 2 (CAP2) is a conserved protein that is found up-regulated in hepatocellular carcinoma (HCC). By using zebrafish, combined with HCC cell lines, we further investigated the role of CAP2. The zebrafish CAP2 sequence was 60% identical to human CAP2 with 77% homology in the C-terminal actin-binding domain, and 58% in the N-terminal cyclase-binding domain. CAP2 expression was observed during zebrafish development and was preferentially expressed in the skeletal muscle and heart. Knockdown using two different morpholinos against CAP2 resulted in a short-body morphant zebrafish phenotype with pericardial edema. CAP2 was observed co-localized with actin in zebrafish skeletal muscle, and in the leading edge of lamellipodium in HCC cell lines. CAP2 silencing resulted in a defect in lamellipodium formation and decreased cell motility in HCC cell lines. Strongly positive expression of CAP2 was observed in 10 of 16 (63%) poorly, 30 of 68 (44%) moderately, and 2 of 21 (10%) well differentiated HCC. CAP2 expression was significantly associated with tumor size, poor differentiation, portal vein invasion, and intrahepatic metastasis. Our results indicate that an important conserved function of CAP2 in higher vertebrates may be associated with the process of skeletal muscle development. CAP2 also played an important role in enhancing cell motility, which may promote a more invasive behavior in the progression of HCC. These findings highlight the link between development and cancer.

Introduction

Hepatocellular carcinoma (HCC) is the sixth most common malignancy in the world and ranks as the third highest cause of cancer-related death globally [1]. HCC is characterized by an obvious multistage process of tumor development, and as with other cancers, diagnosis of early stage HCC is important for appropriate treatment. Previously, we reported that the cyclase-associated protein 2 (CAP2) gene was upregulated in early HCC [2]. CAP was originally identified in the budding yeast, *Saccharomyces cerevisiae*,

*Corresponding author. Fax: +81 3 3353 3290.
E-mail address: msakamot@z5.keio.jp (M. Sakamoto).

0014-4827/$ - see front matter © 2012 Elsevier Inc. All rights reserved.
http://dx.doi.org/10.1016/j.yexcr.2012.09.013

as a factor required for RAS-activated adenylate cyclase activity [3,4], and since then, at least two homologs of CAP, CAP1 and CAP2 have been found in mammals [5–8]. In yeast, the amino (N)-terminal domain of CAP interacts with adenylyl cyclase and is necessary for the cellular response to activate RAS protein. The carboxyl (C)-terminal domain, on the other hand, appears to play a role in nutritional responses and actin distribution, and is necessary for normal cellular morphology [9–11]. Comparing human or rat CAP protein with yeast indicates that only the C-terminal functions of CAP are highly conserved [5,7]. However, the mechanisms underlying actin regulation by CAP are not yet completely understood. The conservation of CAP functional properties in mammals or higher vertebrates suggests that there are still some unrevealed functions of CAP. The CAP homolog, CAP1 is well studied [12,13] compared with CAP2. Interestingly, we found upregulation of CAP2 in early stage HCC [2], and its expression was related to the multistage development of hepatocarcinogenesis [14]. *CAP2* overexpression has not been previously reported in human cancer. Thus, our previous studies indicated an intriguing function of *CAP2* in HCC, as well as in mammals, which requires further exploration.

Recently, the zebrafish (*Danio rerio*) widely used in developmental studies has emerged as a novel vertebrate model to study cancer susceptibility and carcinogenesis, since they offer combined advantages of invertebrate and mammalian models. They have large clutch sizes, and rapid embryonic development. Organogenesis is easy to examine *in vivo* and in real time. High similarities between the histology of normal and malignant zebrafish tissue to that of mouse and human samples has made zebrafish an excellent model system for cancer [15,16]. Also, the ability to perform large-scale 'reverse' genetics using morpholino synthetic anti-sense oligonucleotides which effectively 'knockdown' gene activity in the zebrafish embryo has further popularized their use as a model system [17,18]. The contribution of zebrafish to the cancer field is still growing. Many approaches to induce tumor formation in zebrafish have been established, and non-invasive methods to image tumor development using the transparent adult zebrafish have also recently been developed [19,20]. Thus, zebrafish have now emerged as a new favorite model to study both development and cancer.

In this study, we examined the expression of CAP2 during zebrafish development and utilized morpholino antisense oligonucleotides for protein knockdown studies in zebrafish. We also investigated the functional role of CAP2 using HCC cell lines and further examined CAP2 expression in HCC clinical specimens.

Material and methods

Embryo collection

Zebrafish embryos were obtained by natural mating of RIKEN wild-type zebrafish (*Danio rerio*). Collected embryos were maintained in egg water (5 mM NaCl, 0.17 mM KCl, 0.33 mM $CaCl_2$, 0.33 mM $MgSO_4$, 10^{-5}% methylene blue) at 28.5 °C and embryos were staged using standard morphological criteria [21]. Embryos were gently dechorionated using watchmaker's forceps.

Tissue resection

Adult zebrafish were anesthetized with tricaine (1:20 dilution in clean tank water) and placed on a sponge. Resection was performed under brightfield imaging on a dissection microscope. The incision was made through the ventral body wall and posterior to the heart using microdissection scissors. The brain, eye, heart, abdominal organs, and skeletal muscle were resected using forceps and quickly placed in lysis buffer for Western blot analysis, or frozen in liquid nitrogen for RNA extraction.

Morpholinos and microinjections

Morpholino antisense oligonucleotides were obtained from Gene Tools LLC (Oregon, USA). Two non-overlapping CAP2 antisense morpholinos, and each corresponding five-mispair control morpholinos were designed: (A) ATG-MO (5′-GACGACCAACCAGAGCCTCCA-TAAC-3′), with its control (5′-GAgGAgCAACCACCAcAGCCTCgATt-AC-3′) and (B) UTR-MO (5′-ATATTACCTCAGATGGTGTGGCCCG-3′), with its control (5′-ATtTTACCTgAGATcGTGTaGCgCG-3′). The sequence of CAP1 antisense morpholino was as follows: ATG-MO (5′-ATCTGCCATGCCGTCGCCGTGTGAA-3′), with its five-mispair control (5′-ATgTGCgATGCCcTCGCCcTGTcAA-3′). The sequence used for standard control was 5′-CCTCTTACCTCAGTTACAATTTATA-3′. Morpholino oligonucleotides were stored in 1.0 mM concentration and were diluted to working concentrations in 1 × Danieau's buffer. A dose range of 0.1–1 mM ATG-MO was defined as effective and specific window of concentration which resulted in comparable specific phenotypes. We used 0.3 mM as our choice of morpholino concentration. For the double knockdown approach, CAP2 and CAP1 morpholinos were mixed in a 1:1 ratio (0.3 mM). Fertilized embryos were injected at the 1–8 cell stages into the cytoplasmic streaming of the yolk with 1–2 nL of solution containing either morpholino, or its mispair control. They were allowed to develop in egg water maintained at 28.5 °C. Developed embryos were photographed using a Leica M275 microscope and further evaluated by Western blot and immunohistochemical analysis.

Western blotting

Lysates of HCC cancer cells, adult male zebrafish organs, and zebrafish larva were gently homogenized in lysis buffer (50 mM Tris–HCl (pH 7.4), 250 mM NaCl, 5 mM EDTA, 1% NP-40 (IGEPAL), 10% glycerol, 1 mM DTT, and 25 × protease inhibitor). After determining protein concentrations using the Quant-iT™ Protein Assay Kits (Invitrogen, Eugene, OR), lysates were loaded onto and separated on SDS-PAGE (4–12% Bis-Tris gel; Invitrogen, Carlsbad, CA), and transferred to PVDF membrane using the semi-dry blotting method. The membranes were blocked with 5% nonfat dry milk and probed with our originally raised rabbit polyclonal antibodies against human CAP2 (1/500), CAP1 (1/200) [14], and a mouse monoclonal beta actin antibody (1/1000; Sigma-Aldrich, St. Louis, MO, USA) as a loading control. Horseradish peroxidase-conjugated secondary antibodies were used to probe the membranes and visualized with ECL western blotting detection reagents (GE Healthcare, UK Ltd., Buckinghamshire, UK).

Immunohistochemical analysis

Zebrafish specimens were fixed in 4% paraformaldehyde-PBS at 4 °C overnight and embedded in paraffin tissue section. For staining, slides were deparaffinized and rehydrated, and sections were heated at 120 °C in 0.1 mM Tris–HCl buffer (pH 9.0) for 10 min using an autoclave. The sections were incubated with

rabbit anti-human CAP2 (1/4000), and CAP1 (1/2000), followed by ImmPRESS anti-rabbit Ig Kit secondary antibody (Vector Laboratories, Burlingame, CA). A rabbit immunoglobulin (1/50000; DAKO X0936, Glostrup, Denmark) was used as a negative control. The sections were counterstained with hematoxylin and then mounted. Immunohistochemical staining for HCC clinical specimens was done on formalin-fixed, paraffin-embedded tissue sections according to the methods previously described [14]. Staining analysis was done at least twice. Smooth muscle of the vascular wall served as the internal positive control. We defined CAP2 staining criteria as follows: intensity stronger than or equal to the positive control with more than 50% positive cell in each lesion was scored 2+, while less than 50% positive cell was scored 1+; intensity weaker than the positive control with positive cell more than 50% was also scored 1+, and with positivity less than 50% was considered negative. According to the previous result of CAP2 expression in HCC [14], we used 50% as a cut-off value to divide the HCC cases into high and low positivity group.

Tissue specimens of HCC

HCCs and corresponding non-cancerous liver tissue were obtained from 91 patients with 105 nodules (21 well differentiated (including 9 early), 68 moderately differentiated, and 16 poorly differentiated HCCs) who underwent surgical resection at Keio University Hospital (Tokyo, Japan) between 2003 and 2006. The histological diagnosis was made according to the criteria set by the World Health Organization [22]. This study was approved by the Ethics Committee of Keio University School of Medicine.

Cell culture

The human HCC cell line, PLC/PRF/5, was obtained from the American Type Culture Collection (Manassas, VA). KYN-2 was established as reported previously [23]. All the cells were grown in RPMI 1640 medium supplemented with 10% fetal bovine serum, 100 U/mL penicillin, and 100 μg/mL streptomycin.

Immunocytochemical analysis

PLC/PRF/5 and KYN-2 cells were grown to confluence on glass slides, fixed with 3.7% formaldehyde, and permeabilized with 0.1% Triton X-100 in phosphate buffered saline. The slides were incubated overnight at 4 °C with CAP2 antibody (1/100). After rinsing, the slides were covered with FITC-labeled secondary antibody (Dako, Glostrup, Denmark) with rhodamine-phalloidin and Hoechst 33342 dye (Invitrogen), and visualized using an Axiovert 200 microscope, and AxioCam CCD camera (Carl Zeiss MicroImaging Inc., Tokyo, Japan). For negative control, PLC/PRF/5 was incubated without primary antibody, and visualized using the LSM 510 Meta confocal microscope (Carl Zeiss, Oberkochen, Germany). All staining analysis was done at least twice.

RNA interference and serum stimulation analysis

Two small interfering RNA (siRNA) targeting two CAP2 sequence (siCAP2A and siCAP2B) were synthesized by B-Bridge International, Inc. The target sequences were GGAGUGAACUUCAAGCAUA and GGAGUUGGAAGGAAAGAAA. Cells were cultured until 70–80% confluence onto collagen I-coated six-well plates, and were transfected with siRNA using the DharmaFECT General Transfection Protocol (Dharmacon, Thermo Fisher Scientific, Lafayette, CO, USA). A non-targeting siRNA pool (QIAGEN, Valencia, CA, USA) was used as a negative control. Cells were incubated at 37 °C, 5% CO_2 for 48 h, and to observe lamellipodium formation, the transfectants were serum starved for 24 h. On the following day, the serum was changed with medium supplemented with 10% FBS for 30 min.

Semi-quantitative RT-PCR analysis

Purification of RNA from each zebrafish tissue samples was accomplished by isolation through Isogen (Nippon Gene Co. LTD, Toyama, Japan), and cDNA was synthesized using the PrimeScript RT reagent Kit (Takara Bio, Shiga, Japan). As a template for amplification, 10 μL of each sample was used. A primer set designed for zebrafish CAP2 expression amplified a 175 base pair fragment (5′-GGCTGATTGATCTGCCTCCTC-3′ and 5′-AAGCACAGTGGGTCTGGGG-3′), and a primer set targeting zebrafish CAP1 amplified a 179 base pair fragment (5′-GATGGCTGCCACGTGTACCT-3′ and 5′-ATCTCGGTGGCTGTGGTGAC-3′). Each reaction was run on 2% agarose in 1 × TAE buffer.

Migration assay

PLC/PRF/5 and KYN-2 cells transfected for 48 h with siCAP2A, siCAP2B, and negative control siRNA were suspended in medium supplemented with 0.5% FBS. Cells treated with each siRNA were dispersed in each of three independent upper chambers of BD BioCoat Control Culture Inserts (pore size=8 μm; BD Biosciences, San Diego, CA, USA). Chemoattractant medium containing 10% FBS was added to the bottom plate. After 24 h incubation, non-migrated cells were removed by scrubbing with cotton-tipped swabs and migrated cells were stained with Diff-Quick stain (Kokusai Shiyaku, Kobe, Japan). The number of migrated cells on three independent membranes was counted under microscope. The ratio of the number of migrated cells represents the mean number of migrated cells with each siRNA treatment, divided by the mean number of migrated control cells.

Statistical analysis

The chi-squared test was used when appropriate to determine the correlations between clinicopathological variables and CAP2 expression. Statistical significance was defined as $P<0.005$. All statistical analyses were carried out using SPSS statistical software (SPSS, Chicago, IL, USA).

Results

CAP2 is expressed in both the embryo and adult zebrafish

The conservation of CAP2 from yeast to mammals suggests that CAP2 also exists in zebrafish. We examined CAP2 presence in zebrafish and found that the zebrafish Cap2 sequence (LOC393809; NP_957130.1) was 60% identical to the already known human CAP2, with 77% homology in the C-terminal actin-binding domain, 57% in the middle proline-rich sequence, and 59% in the N-terminal

domain (Fig. 1A). Although all three domains of CAP were conserved, homologies in the C-terminal actin-binding domain were higher than other regions. By immunohistochemical analysis, CAP2 expression could be observed in 24 h post-fertilization (hpf) embryo, and continued in the larva and adult zebrafish. In the early embryo development (Fig. 1B), CAP2 was seen in the neural tube (nt), and a group of tissues that will give rise to a muscle segment, the myotome (my). As the embryo developed to larva, CAP2 expression was observed in the brain (br), and skeletal muscle (sk). In adult zebrafish tissue, CAP2 expression was also observed in the brain, heart and skeletal muscle (Fig. 1C and D). We also compared the expression of CAP2 and CAP1, a homolog of CAP2 that also has been identified in zebrafish [24,25]. Differential expression of CAP2 was particularly observed in the heart and skeletal muscle, where CAP2 was highly expressed (Supplementary Fig. 1A).

CAP2 zebrafish morphants showed an abnormal short-body phenotype

To study CAP2 function in zebrafish, we created CAP2 knockdown morphants by injecting CAP2 antisense morpholino oligonucleotides into cytoplasmic streaming of 1- to 8-cell stage zebrafish embryos. To assess specificity, two non-overlapping morpholinos (A and B) were designed against a CAP2 sequence, with five-mispair control oligo for each morpholino as a negative

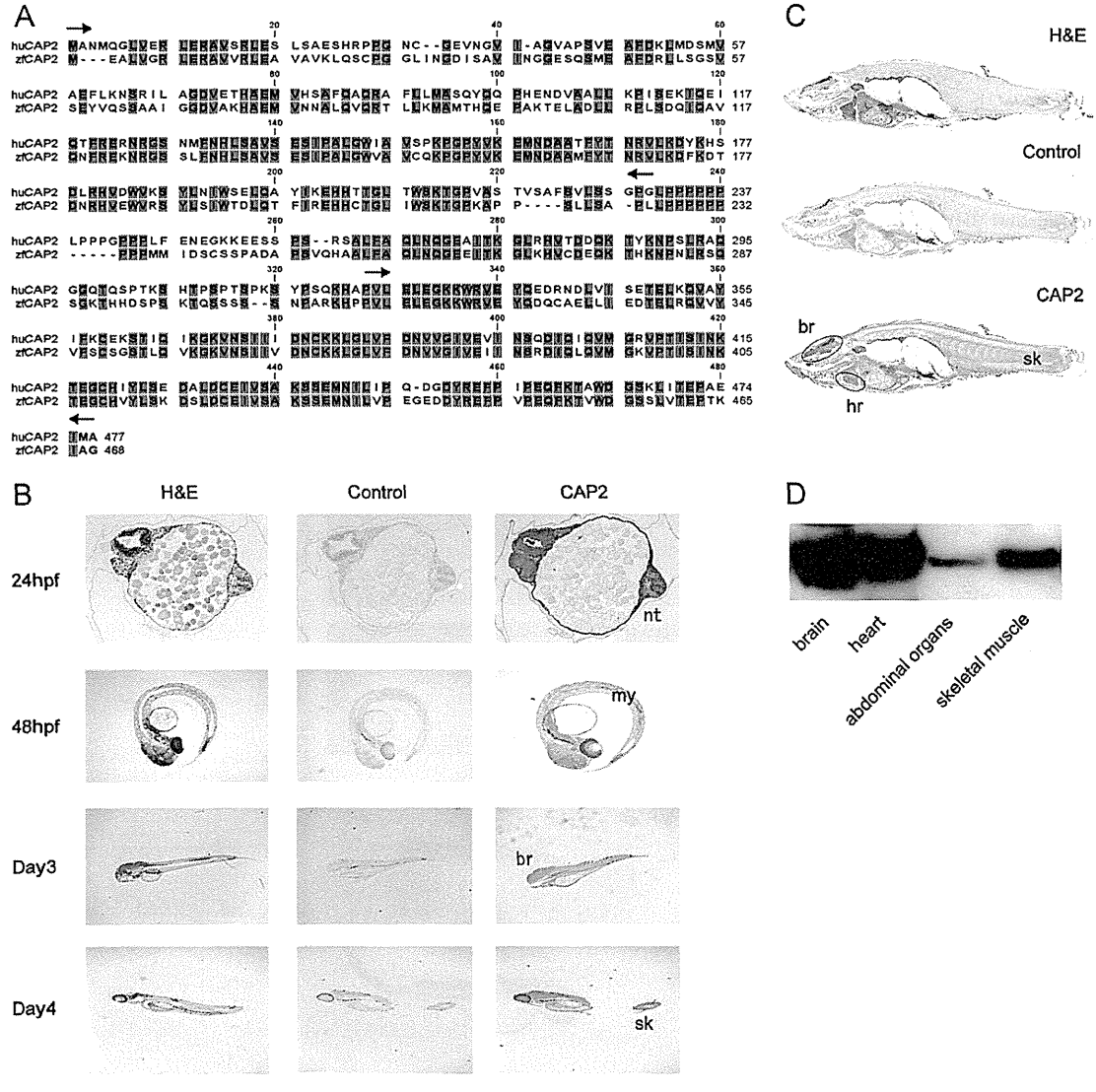

Fig. 1 – Cyclase-Associated Protein 2 (CAP2) is expressed in both embryo and adult zebrafish. (A) Direct amino acid comparison between human and zebrafish CAP2 sequences, with conserved amino acids highlighted in red. The N-terminal domain is depicted by black arrows, C-terminal domain is depicted by red arrows, and between them is a proline-rich sequence. (B) CAP2 expression in zebrafish embryo, 24 and 48 hpf, followed by day 3 and day 4 larva. CAP2 was expressed in the neural tube (nt) and in the myotome (my) of a 48 hpf embryo. In day 3 and day 4 larva, CAP2 was expressed in the brain (br) and skeletal muscle (sk). (C) CAP2 expression in adult male zebrafish was observed in the brain, heart (hr) and skeletal muscle. Negative control was included in each staining. (D) Protein expression was confirmed with Western blot analysis. (For interpretation of the references to color in this figure legend, the reader is referred to the web version of this article.)

control. Injecting either CAP2 morpholinos resulted in reproducible and identical morphants phenotypes. In 24 hpf, we observed that most of the morphants embryos (MO A, B) showed shorter body length compared with the mispaired control (MP A, B) (Fig. 2A). Additional controls using tracer injected embryos (PR) as well as wild-type embryos (WT) did not show an abnormal phenotype (Fig. 2A). CAP2 morphant embryos also displayed pericardial edema with persistently short-body phenotype at three days post-fertilization, while the mispair control embryos developed similarly to the wild-type (Fig. 2B). To make sure that the experiment is being performed in the effective and specific concentration range, injection of the CAP2 targeted morpholino was performed side-by-side with the five-mispair control oligo, and the resulting short-body phenotype was observed in a concentration-dependent manner (Table 1). At least two independent injection experiments were replicated. Reduced CAP2 expression was observed in CAP2 knockdown morphant embryos with immunohistochemical analysis (Fig. 2C). The morphants were mostly non-motile and did not survive due to stalled development. Additional control using 0.3 mM standard control oligo which has been known can be extensively used without triggering off-target effects showed that the resulting short-body phenotype could be reduced until 17% (Supplementary Table 1). Since CAP1 was also ubiquitously expressed in zebrafish, we performed double knockdown experiments by mixing both of the two sequences of CAP2 and CAP1 morpholinos. Similar short-body phenotype was observed, and a clear reduction of both CAP2 and CAP1 expression was obtained in Western blot analysis (Supplementary Fig. 1B). The number of morphant short-body embryos was not enhanced by the double knockdown strategy (Table 1), suggesting no interference between each other.

CAP2 colocalized with actin both in zebrafish and HCC cell lines

Both CAP2 and CAP1 protein were detected from the zebrafish larval period, however, clear strong expression of CAP2 was particularly observed in the skeletal muscle area, while only thin weak expression of CAP1 was observed in the same area of skeletal muscle. Immunostaining using antibody against muscle actin and alpha-sarcomeric actin, i.e., it only reacts with skeletal muscle actin, also showed a strong clear expression of actin in the zebrafish skeletal muscle area, where CAP2 was also expressed. They both showed a similar expression pattern suggesting colocalization of CAP2 and actin in the skeletal muscle of zebrafish (Fig. 3A, Supplementary Fig. 1C). These findings indicate the possibility that the abnormal short-body phenotype seen in the CAP2 zebrafish morphants may be due to the downregulation of actin-associated CAP2. We also investigated colocalization of CAP2 and actin in human cancer cells. According to our previous report, CAP2 was highly expressed in multistage hepatocarcinogenesis, and we frequently found that the tumor cells invading the stroma were clearly stained with CAP2 [14]. In the present study, we found that CAP2 was highly distributed in the perinuclear area, and was also co-localized with actin in the leading edge of lamellipodium in PLC/PRF/5, and

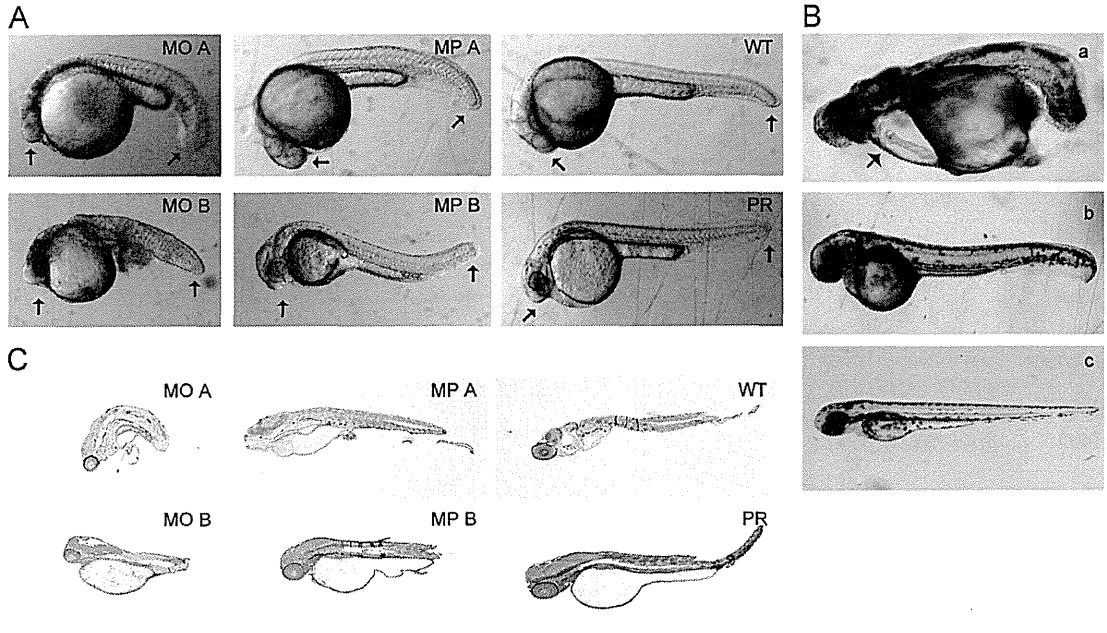

Fig. 2 – Cyclase-associated protein 2 (CAP2) zebrafish morphants showed a short-body phenotype. (A) Shorter body length was observed in morphant-A and morphant-B CAP2 embryos (MO A, MO B) compared with each five-mispair negative control (MP A, MP B), wild-type control (WT), and additional injection controls using embryos injected only with the tracer, phenol red (PR). Black arrows mark the length boundary. (B) The resulting short-body phenotype was persistently observed with pericardial edema (red arrow) at 3 days post fertilization (a), while developmental defects were not observed in morphant controls (b) or wild-type embryos (c). All morphants were injected with 0.3 mM concentration of morpholino. (C) At 5 days post fertilization, immunohistochemical analysis showed reduced expression of CAP2 in both morphants, compared with the mispair controls and wild-type or tracer control embryos. (For interpretation of the references to color in this figure legend, the reader is referred to the web version of this article.)

Table 1 – Concentration-dependence effect of cyclase-associated protein2 (CAP2) morpholinos on early development of zebrafish embryos.

Injections	Embryos injected	Eggs left after 24 h	Normal	Short-body	Percentage showing phenotype
0.1 mM (MO-A)[a]	59	52	41	11	21
0.1 mM (MP-A)[b]	68	61	56	5	8
0.3 mM (MO-A)	154	78	12	66	85
0.3 mM (MP-A)	94	37	25	12	32
0.5 mM (MO-A)	82	35	3	32	91
0.5 mM (MP-A)	86	41	26	15	37
1 mM (MO-A)	118	10	3	7	70
1 mM (MP-A)	120	55	15	40	73
0.3 mM (MO-B)[c]	68	60	3	57	95
0.3 mM (MP-B)[d]	69	62	55	7	11
CAP2A+ CAP1 (MO)	59	26	2	24	92
CAP2A+CAP1 (MP)	83	54	19	35	65
CAP2B+CAP1 (MO)	75	56	7	49	88
CAP2B+CAP1 (MP)	76	54	39	15	28

[a] Antisense morpholino A.
[b] Mispaired control A.
[c] Antisense morpholino B.
[d] Mispaired control B.

the highly metastatic, KYN-2, HCC cell lines (Fig. 3B, Supplementary Fig. 2). These findings suggest that the role of CAP2 in inducing stromal invasion may relate to its actin cytoskeletal function.

CAP2 silencing in HCC cell lines resulted in a defect in lamellipodium formation and a reduction in cell motility

We further assessed the role of CAP2 in relation to its cytoskeletal function. CAP2 knockdown was performed in HCC cell lines using two small interfering RNA molecules (siCAP2 A and siCAP2B). The knockdown effect was confirmed using Western blot analysis (Fig. 4A), and the transfected cells were serum starved for 24 h before stimulation with serum the next day. Within 15 min after serum stimulation, control cells started to spread out and extended lamellipodium around the circumference of the cell clusters. Lamellipodium formation in CAP2-knockdown cells was, however, still restrained or only partial (Fig. 4B). The role of CAP2 in cell motility was evaluated by migration assay with CAP2-knockdown cells. The number of migrating CAP2-knockdown cells decreased compared with the controls (Fig. 4C). We did not observe reduced cell proliferation in CAP2-knockdown cells (data not shown), suggesting that the decreased number of migrated cells was solely due to the reduced cell motility caused by CAP2 knockdown.

CAP2 expression in HCC clinical cases correlated with tumor size, poor differentiation, portal vein invasion, and intrahepatic metastasis

We evaluated CAP2 expression in 105 HCC nodules (21 well differentiated (including 9 early), 68 moderately differentiated, and 16 poorly differentiated HCCs). Immunohistochemical evaluation was done by combining the intensity and positivity of CAP2 staining (Supplementary Fig. 3). Strongly positive expression of CAP2 was mostly observed in progressed HCC. A 2+ score was observed in 10 of the 16 (63%) poorly differentiated HCCs, 30 of the 68 (44%) moderately differentiated HCCs, and 2 of the 21 (10%) well differentiated HCCs (none of the early nodules had 2+ score). Reversely, negative expression was observed in only 2 of the 16 (13%) poorly differentiated HCCs, 3 of the 68 (4%) moderately differentiated HCCs, and 10 of the 21 (48%) well differentiated HCCs (including 6 of the 9 early nodules (67%)) (Table 2). CAP2 expression was significantly associated with tumor size ($P=0.004$), poor differentiation ($P=0.001$), portal vein invasion ($P=0.001$), and intrahepatic metastasis ($P=0.002$) (Table 3).

Discussion

Cyclase-associated protein, CAP, has been identified as a bifunctional protein from yeast through mammals, indicating the retention of important conserved functions during evolution. A homolog of yeast CAP, which is required for proper genesis of cell polarity in eukaryotes, has been identified in *Drosophila*. Loss of *Drosophila* CAP causes cell polarity defects, altering the distribution of actin filaments and resulting in various developmental defects [26]. CAP knockout mutant *Dictyostelium* cells showed changes in cell polarity, F-actin organization, and phototaxis suggesting that CAP may play a critical part in cell polarity and movement of diverse organisms [27]. In human and adult rat tissue, at least two different homologs of CAP, CAP1 and CAP2, have been found, and they share more than 60% amino acid identity [5,6,8]. However, the functions of CAPs in mammals or higher vertebrates are not well established, and in particular, studies on CAP2 are lacking. In the zebrafish, the gene encoding CAP1 has been reported and shares 63% identity with human CAP1 [24]. In the present study, we identified a CAP2 protein which shares 60% identity with human CAP2. Although both CAPs are conserved in zebrafish, their expression pattern is different. We observed that CAP2 was expressed in the brain,

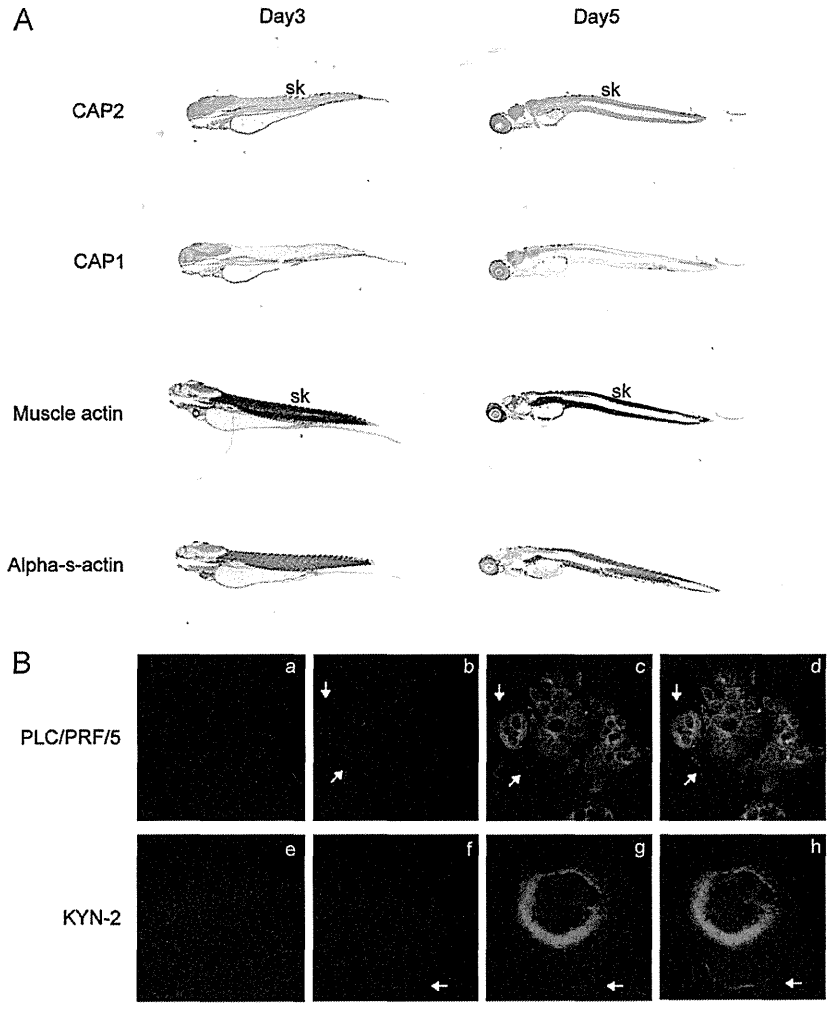

Fig. 3 – Cyclase-associated protein 2 (CAP2) observed co-localized with actin in zebrafish and hepatocellular carcinoma (HCC) cell lines. (A) Day 3 and day 5 of zebrafish larva with CAP2, CAP1 and actin immunostaining. CAP2 was highly expressed in the skeletal muscle area compared with CAP1. Immunostaining of muscle actin and alpha-sarcomeric actin was also observed in the zebrafish skeletal muscle area, suggesting co-localization of skeletal muscle actin and CAP2, magnification 20×. (B) Immunocytochemistry of PLC/PRF/5 and KYN-2 HCC cell lines. CAP2 expression was observed co-localized with the lamellipodium as a characteristic feature of motile cells, marked by white arrow (a,e, Hoechst: blue; b,f, anti-phalloidin-rhodamine: red; c,g, anti-CAP2: green; d,h, merged). (For interpretation of the references to color in this figure legend, the reader is referred to the web version of this article.)

and was particularly expressed in the heart and skeletal muscle. This is in accordance with previous reports showing that CAP1 is widely expressed in nearly all organs, while CAP2 expression is localized in the brain, heart, and skeletal muscle in rat tissue [8,28]. In mouse embryonic development, the expression of CAP2 is highly restricted to the developing muscle tissues and heart [12]. A new report has shown CAP2 expression in the cardiac primordial and in the leading edge of the myotome during early *Xenopus* embryogenesis [29]. We found that knockdown of CAP2 expression in the zebrafish resulted in a shorter body compared with the control embryos. There was an abundant original expression and a co-localization of CAP2 and actin in the zebrafish skeletal muscle. CAP2 appears to act as a striated muscle-specific protein during zebrafish development. Thus, the short-body phenotype with pericardial edema observed after CAP2 knockdown in zebrafish was likely caused by the down regulation of actin-associated CAP2. This indicates that CAP2 plays an important conserved role in higher vertebrates, particularly in the development of skeletal muscle. We realized that almost all knockdowns of various genes in zebrafish affect body development [30–32], through skeletal muscle, somite, or neural formation defects, indicating that many genes or signaling pathways are involved in the patterning processes in a vertebrate embryo; here we showed the possible role of CAP2. Further, it would be interesting to investigate the mechanisms regulating CAP2 and CAP1 in developmental processes and in different organs.

Previously, using oligonucleotides array technology we identified *CAP2* as one of the genes upregulated in early HCC [2]. Overexpression of CAP2 was observed in a stepwise manner

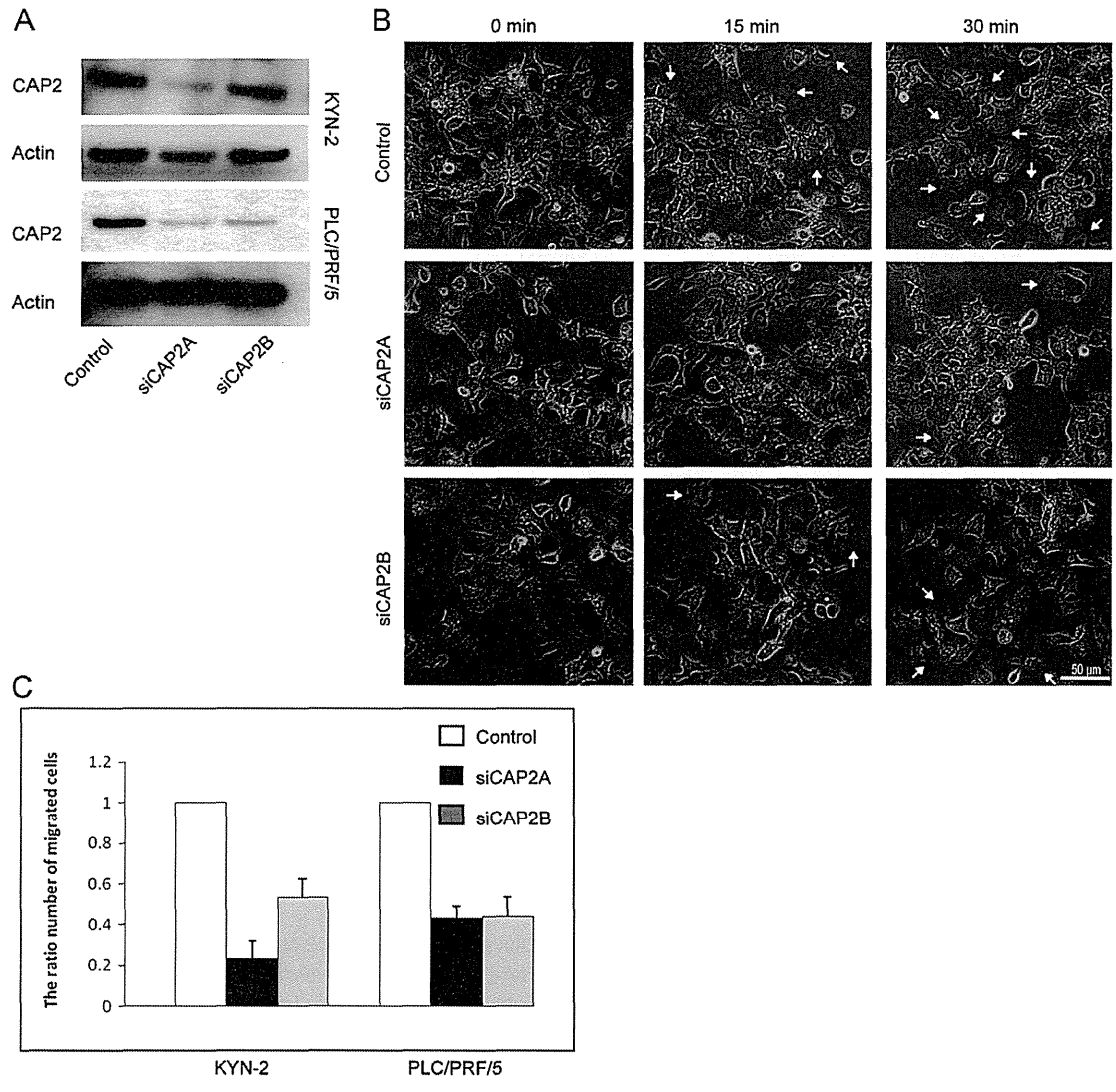

Fig. 4 – Cyclase-associated protein 2 (CAP2) silencing affected lamellipodium formation and cell migration. (A) Western blot analysis to confirm the suppression of CAP2 in KYN2 and PLC/PRF/5 cell lines. (B) Serum stimulation analysis of KYN-2 cells. After serum-starving (0 min), the lamellipodium of control cells was soon established following serum-stimulation (15 and 30 min) compared with the CAP2-knockdown cells, siCAP2A and siCAP2B. White arrows indicated the lamellipodium formation. Scale bar=50 μm. (C) Migration assay showing a reduction in the migration of both KYN-2 and PLC/PRF/5 cells, compared with the control cells. The ratio of the number of migrated cells represents the mean number (under microscope observation) of migrated cells per field against control cells. Bars reveal standard error of the mean (SEM).

during the progression of HCC and interestingly, in early HCC, the tumor cells invading the stroma stained positive for CAP2 and were clearly highlighted [14]. Here, we further investigated the co-localization of CAP2 and actin in the leading edge of the lamellipodium of HCC cells. Extension of the lamellipodium following serum stimulation was inhibited, and cell motility was reduced in CAP2 knockdown cells. This suggests CAP2 involvement in remodeling of the actin filament that occurs at the leading edge of lamellipodium as a characteristic feature of motile cells. The polymerization of actin is essential for motile processes and is regulated by some signaling pathway for actin-binding protein [33,34]. Thus, CAP2 seems to play a role in cell motility, resulting in promoting skeletal muscle development, and stromal invasion in early HCC. Moreover, we observed a significant correlation between overexpression of CAP2 and progressed features in HCC, such as tumor size, poor differentiation, portal vein invasion, and intrahepatic metastasis. This suggests that CAP2 overexpression is involved in promoting the invasive behavior of HCC cells. The role of CAP2 in other human cancers is, however, not yet clear. Human CAP2 can also interact with CAP1 and actin [35]. We have reported that the overexpression of CAP1 in pancreatic cancers is also related to the aggressive behavior of pancreatic cancer cells [36]. Further investigation of cellular and molecular mechanisms governing CAP2 role in cell migration ability is necessary to expand our knowledge on how actin dynamics is controlled. Elucidating the

Table 2 – Immunohistochemical analysis of cyclase-associated protein (CAP2) in hepatocellular carcinoma (HCC) (n=105).

Histology	CAP2 staining score		
	2+	1+	–
Well differentiated HCC (n=21)	2(10%)	9(43%)	10(48%)
Early HCC (n=9)	0(0%)	3(33%)	6(67%)
Moderately differentiated (n=68)	30(44%)	35(51%)	3(4%)
Poorly differentiated (n=16)	10(63%)	4(25%)	2(13%)

Table 3 – Correlations between clinicopathological characteristics and cyclase-assoicated protein 2 (CAP2) expression in HCC clinical cases.

Characteristics	CAP2 expression		
	–, 1+	2+	P value
Mean age (years)			NA[a]
Gender			0.810
Male	51	36	
Female	10	8	
Etiology			
Hepatitis B virus			0.010
Negative	51	27	
Positive	10	17	
			0.052
Negative	23	25	
Positive	38	19	
AFP serum level (ng/ml)			0.492
<20	36	23	
≧20	25	21	
Fibrosis			0.073
Liver cirrhosis	24	23	
Others	37	17	
Tumor size (cm)			0.004
<2.0	24	6	
≧2.0	37	38	
Tumor differentiation			0.001
Well (early)	19(9)	2(0)	
Moderately	37	31	
Poorly	5	11	
Portal involvement			0.001
–	37	12	
+	24	32	
Intrahepatic metastasis			0.002
–	53	27	
+	8	17	

[a] Not available.

conserved collaborative role of CAP2 and CAP1, and whether they interact with the RAS signaling pathway may also reveal their role in human cancers. Additionally, the use of zebrafish to study hepatocarcinogenesis offers a new innovative research approach [37]. A previous report has shown conserved gene expression profiles between human and zebrafish liver cancer [38]. Future studies on how CAP2 functions in zebrafish liver are necessary to advance our understanding of hepatocarcinogenesis. Combining developmental and cancer studies will provide an exciting future framework to understand how development and carcinogenesis are linked.

In summary, we showed that CAP2 has an important conserved function across species. In zebrafish, the role of CAP2 appears to be associated with the developmental process, particularly in skeletal muscle development. In HCC, CAP2 was associated with enhanced cell motility, and was involved in the progression of HCC. The role of CAP2 in the developmental process of higher vertebrates as well as in human liver cancer is shedding some light on the progress issue of development and cancer.

Conflict of interest

The authors declare there is no conflict of interest regarding this study.

Acknowledgments

Our sincere thanks to H. Suzuki, Y. Hashimoto, M. Suzuki, and K. Nakajima, for providing technical assistance. Also, to M. Ono for her help and support at Keio University Small Fish Center (KSFC). This work was supported by a Grant-in-aid for Scientific Research (B) from the Ministry of Education, Culture, Sports, Science, and Technology (MEXT) of Japan; Grants for the Health Labor Sciences Research and the Third Term Comprehensive 10-Year Strategy for Cancer Control from the Ministry of Health, Labor and Welfare of Japan; Grant-in-aid from The Vehicle Racing Commemorative Foundation. This study was performed as a research program of the Project for Development of Innovative Research on Cancer Therapeutics (P-Direct) from the Ministry of Education, Culture, Sports, Science and Technology of Japan.

Appendix A. Supporting information

Supplementary data associated with this article can be found in the online version at http://dx.doi.org/10.1016/j.yexcr.2012.09.013.

REFERENCES

[1] D.M. Parkin, F. Bray, J. Ferlay, P. Pisani, Global cancer statistics, 2002, CA Cancer J. Clin. 55 (2005) 74–108.
[2] M. Chuma, M. Sakamoto, K. Yamazaki, T. Ohta, M. Ohki, M. Asaka, S. Hirohashi, Expression profiling in multistage hepatocarcinogenesis: identification of HSP70 as a molecular

marker of early hepatocellular carcinoma, Hepatology 37 (2003) 198–207.
[3] J. Field, A. Vojtek, R. Ballester, G. Bolger, J. Colicelli, K. Ferguson, J. Gerst, T. Kataoka, T. Michaeli, S. Powers, M. Riggs, L. Rodgers, I. Wieland, B. Wheland, M. Wigler, Cloning and characterization of CAP, the *S. cerevisiae* gene encoding the 70 kd adenylyl cyclase-associated protein, Cell 61 (1990) 319–327.
[4] M. Fedor-Chaiken, R.J. Deschenes, J.R. Broach, SRV2, a gene required for RAS activation of adenylate cyclase in yeast, Cell 61 (1990) 329–340.
[5] H. Matviw, G. Yu, D. Young, Identification of a human cDNA encoding a protein that is structurally and functionally related to the yeast adenylyl cyclase-associated CAP proteins, Mol. Cell. Biol. 12 (1992) 5033–5040.
[6] G. Yu, J. Swiston, D. Young, Comparison of human CAP and CAP2, homologs of the yeast adenylyl cyclase-associated proteins, J. Cell Sci. 107 (Pt 6) (1994) 1671–1678.
[7] A. Zelicof, J. Gatica, J.E. Gerst, Molecular cloning and characterization of a rat homolog of CAP, the adenylyl cyclase-associated protein from *Saccharomyces cerevisiae*, J. Biol. Chem. 268 (1993) 13448–13453.
[8] J. Swiston, A. Hubberstey, G. Yu, D. Young, Differential expression of CAP and CAP2 in adult rat tissues, Gene 165 (1995) 273–277.
[9] J.E. Gerst, K. Ferguson, A. Vojtek, M. Wigler, J. Field, CAP is a bifunctional component of the *Saccharomyces cerevisiae* adenylyl cyclase complex, Mol. Cell. Biol. 11 (1991) 1248–1257.
[10] A. Vojtek, B. Haarer, J. Field, J. Gerst, T.D. Pollard, S. Brown, M. Wigler, Evidence for a functional link between profilin and CAP in the yeast *S. cerevisiae*, Cell 66 (1991) 497–505.
[11] F. Shima, T. Okada, M. Kido, H. Sen, Y. Tanaka, M. Tamada, C.D. Hu, Y. Yamawaki-Kataoka, K. Kariya, T. Kataoka, Association of yeast adenylyl cyclase with cyclase-associated protein CAP forms a second Ras-binding site which mediates its Ras-dependent activation, Mol. Cell. Biol. 20 (2000) 26–33.
[12] E. Bertling, P. Hotulainen, P.K. Mattila, T. Matilainen, M. Salminen, P. Lappalainen, Cyclase-associated protein 1 (CAP1) promotes cofilin-induced actin dynamics in mammalian nonmuscle cells, Mol. Biol. Cell 15 (2004) 2324–2334.
[13] K. Moriyama, I. Yahara, Human CAP1 is a key factor in the recycling of cofilin and actin for rapid actin turnover, J. Cell Sci. 115 (2002) 1591–1601.
[14] R. Shibata, T. Mori, W. Du, M. Chuma, M. Gotoh, M. Shimazu, M. Ueda, S. Hirohashi, M. Sakamoto, Overexpression of cyclase-associated protein 2 in multistage hepatocarcinogenesis, Clin. Cancer Res. 12 (2006) 5363–5368.
[15] J.F. Amatruda, J.L. Shepard, H.M. Stern, L.I. Zon, Zebrafish as a cancer model system, Cancer Cell 1 (2002) 229–231.
[16] W. Goessling, T.E. North, L.I. Zon, New waves of discovery: modeling cancer in zebrafish, J. Clin. Oncol. 25 (2007) 2473–2479.
[17] A. Nasevicius, S.C. Ekker, Effective targeted gene 'knockdown' in zebrafish, Nat. Genet. 26 (2000) 216–220.
[18] D.R. Corey, J.M. Abrams, Morpholino antisense oligonucleotides: tools for investigating vertebrate development, Genome Biol. 2 (2001) (REVIEWS1015).
[19] K. Stoletov, R. Klemke, Catch of the day: zebrafish as a human cancer model, Oncogene 27 (2008) 4509–4520.
[20] R.M. White, A. Sessa, C. Burke, T. Bowman, J. LeBlanc, C. Ceol, C. Bourque, M. Dovey, W. Goessling, C.E. Burns, L.I. Zon, Transparent adult zebrafish as a tool for in vivo transplantation analysis, Cell Stem Cell 2 (2008) 183–189.
[21] C.B. Kimmel, W.W. Ballard, S.R. Kimmel, B. Ullmann, T.F. Schilling, Stages of embryonic development of the zebrafish, Dev. Dyn. 203 (1995) 253–310.
[22] S. Hirohashi, K. Ishak, M. Kojiro, I. Wanless, N.D. Theise, H. Tsukuma, Tumours of the liver and intrahepatic bile ducts, in: S.R. Hamilton, L.A. Aaltonen (Eds.), Pathology and Genetics of Tumours of the Digestive System, IARC Press, Lyon, 2000, pp. 157–202.
[23] T. Genda, M. Sakamoto, T. Ichida, H. Asakura, M. Kojiro, S. Narumiya, S. Hirohashi, Cell motility mediated by rho and Rho-associated protein kinase plays a critical role in intrahepatic metastasis of human hepatocellular carcinoma, Hepatology 30 (1999) 1027–1036.
[24] D.F. Daggett, C.A. Boyd, P. Gautier, R.J. Bryson-Richardson, C. Thisse, B. Thisse, S.L. Amacher, P.D. Currie, Developmentally restricted actin-regulatory molecules control morphogenetic cell movements in the zebrafish gastrula, Curr. Biol. 14 (2004) 1632–1638.
[25] D.F. Daggett, C.R. Domingo, P.D. Currie, S.L. Amacher, Control of morphogenetic cell movements in the early zebrafish myotome, Dev. Biol. 309 (2007) 169–179.
[26] B. Baum, W. Li, N. Perrimon, A cyclase-associated protein regulates actin and cell polarity during *Drosophila* oogenesis and in yeast, Curr. Biol. 10 (2000) 964–973.
[27] A.A. Noegel, R. Blau-Wasser, H. Sultana, R. Muller, L. Israel, M. Schleicher, H. Patel, C.J. Weijer, The cyclase-associated protein CAP as regulator of cell polarity and cAMP signaling in *Dictyostelium*, Mol. Biol. Cell 15 (2004) 934–945.
[28] V. Peche, S. Shekar, M. Leichter, H. Korte, R. Schroder, M. Schleicher, T.A. Holak, C.S. Clemen, Y.B. Ramanath, G. Pfitzer, I. Karakesisoglou, A.A. Noegel, CAP2, cyclase-associated protein 2, is a dual compartment protein, Cell. Mol. Life Sci. 64 (2007) 2702–2715.
[29] M. Wolanski, F. Khosrowshahian, L. Jerant, I.S. Jap, J. Brockman, M.J. Crawford, Expression of CAP2 during early *Xenopus* embryogenesis, Int. J. Dev. Biol. 53 (2009) 1063–1067.
[30] S. Sumanas, H.J. Kim, S. Hermanson, S.C. Ekker, Zebrafish frizzled-2 morphant displays defects in body axis elongation, Genesis 30 (2001) 114–118.
[31] D.J. Mawdsley, H.M. Cooper, B.M. Hogan, S.H. Cody, G.J. Lieschke, J.K. Heath, The Netrin receptor Neogenin is required for neural tube formation and somitogenesis in zebrafish, Dev. Biol. 269 (2004) 302–315.
[32] S.C. Little, M.C. Mullins, Twisted gastrulation promotes BMP signaling in zebrafish dorsal–ventral axial patterning, Development 131 (2004) 5825–5835.
[33] T.P. Loisel, R. Boujemaa, D. Pantaloni, M.F. Carlier, Reconstitution of actin-based motility of *Listeria* and *Shigella* using pure proteins, Nature 401 (1999) 613–616.
[34] T.D. Pollard, L. Blanchoin, R.D. Mullins, Molecular mechanisms controlling actin filament dynamics in nonmuscle cells, Annu. Rev. Biophys. Biomol. Struct. 29 (2000) 545–576.
[35] A. Hubberstey, G. Yu, R. Loewith, C. Lakusta, D. Young, Mammalian CAP interacts with CAP, CAP2, and actin, J. Cell. Biochem. 61 (1996) 459–466.
[36] K. Yamazaki, M. Takamura, Y. Masugi, T. Mori, W. Du, T. Hibi, N. Hiraoka, T. Ohta, M. Ohki, S. Hirohashi, M. Sakamoto, Adenylate cyclase-associated protein 1 overexpressed in pancreatic cancers is involved in cancer cell motility, Lab. Invest. 89 (2009) 425–432.
[37] J. Chu, K.C. Sadler, New school in liver development: lessons from zebrafish, Hepatology 50 (2009) 1656–1663.
[38] S.H. Lam, Y.L. Wu, V.B. Vega, L.D. Miller, J. Spitsbergen, Y. Tong, H. Zhan, K.R. Govindarajan, S. Lee, S. Mathavan, K.R. Murthy, D.R. Buhler, E.T. Liu, Z. Gong, Conservation of gene expression signatures between zebrafish and human liver tumors and tumor progression, Nat. Biotechnol. 24 (2006) 73–75.

Toshiya Kamiyama

Identification of novel serum biomarkers of hepatocellular carcinoma using glycomic analysis

Toshiya Kamiyama, MD[1)], Hideki Yokoo, MD[1)], Jun-Ichi Furukawa[3)], Masaki Kurogochi[3)], Tomoaki Togashi[3)], Nobuaki Miura[3)], Kazuaki Nakanishi, MD[2)], Hirofumi Kamachi, MD[1)], Tatsuhiko Kakisaka, MD[1)], Yosuke Tsuruga, MD[1)], Masato Fujiyoshi, MD[1)], Akinobu Taketomi, MD[1)], Shin-Ichiro Nishimura[3)], and Satoru Todo, MD[1)]

The Department of Gastroenterological Surgery I[1)] and the Department of Transplantation Surgery[2)], Hokkaido University Graduate School of Medicine

Graduate School of Life Science and Frontier Research Center for the Post-Genome Science and Technology[3)], Hokkaido University

Address for correspondence:

Toshiya Kamiyama, MD.
The Department of Gastroenterological Surgery I
Hokkaido University Graduate School of Medicine
North 15, West 7, Kita-ku, Sapporo 060-8638 Japan
Phone: +81-11-706-5923 Fax: +81-11-717-7515
E-mail: t-kamiya@med.hokudai.ac.jp

Running Title: New biomarkers of hepatocellular carcinoma determined by glycomics

This article has been accepted for publication and undergone full peer review but has not been through the copyediting, typesetting, pagination and proofreading process which may lead to differences between this version and the Version of Record. Please cite this article as an 'Accepted Article', doi: 10.1002/hep.26262

Key words: hepatocellular carcinoma; glycomics; hepatectomy; biomarker.

Conflicts of interest

The authors declare no conflicts of interest.

Abstract

Background: The altered *N*-glycosylation of glycoproteins has been suggested to play an important role in the behavior of malignant cells. Using novel glycomics technology, we attempted to determine the specific and detailed *N*-glycan profile for hepatocellular carcinoma (HCC) and investigate the prognostic capabilities.

Method: From 1999 to 2011, 369 patients underwent primary curative hepatectomy in our facility and were followed up for a median of 60.7 months. As normal controls, Japanese 26 living related liver transplantation donors were selected not infected by hepatitis B and C virus. Their mean age was 40.0. Fifteen (57.7%) were male. We used a glycoblotting method to purify *N*-glycans from preoperative blood samples from this cohort (10μl serum) which were then identified and quantified using mass spectrometry (MS). Correlations between the *N*-glycan levels and the clinicopathologic characteristics and outcomes for these patients were evaluated.

Results: Our analysis of the relative areas of all the sugar peaks identified by MS, totaling 67 *N*-glycans, revealed that a proportion had higher relative areas in the HCC cases compared with the normal controls. Fourteen of these molecules had an area under the curve of greater than 0.80. Analysis of the correlation between these 14 *N*-glycans and surgical outcomes by univariate and multivariate analysis identified G2890 (*m/z* value, 2890.052) as significant recurrent factor and G3560 (*m/z* value,

3560.295) as significant prognostic factor. G2890 and G3560 were found to be strongly correlated with tumor number, size and vascular invasion.

Conclusion: Quantitative glycoblotting based on whole serum *N*-glycan profiling is an effective approach to screening for new biomarkers. The G2890 and G3560 *N*-glycans determined by tumor glycomics appear to be promising biomarkers for malignant behavior in HCCs.

Abbreviations

HCC: hepatocellular carcinoma

PS: patient Survival

DFS: disease-free survival

RF: risk factor

ICGR15: indocyanin green retention rate at 15 minutes

AFP: alpha-fetoprotein

PIVKA-II: protein induced by vitamin K absence or antagonism factor II

AFP-L3: Lens culinaris agglutinin-reactive fraction of alpha-fetoprotein

AUC: area under the curve

ROC: receiver operating characteristics

Introduction

Hepatocellular carcinoma (HCC) is a common and fatal malignancy with a worldwide occurrence (1). Liver resection has shown the highest level of control among the local treatments for HCC and is associated with a good survival rate (2, 3). However, the recurrence rates for HCC are still high even when a curative hepatectomy is performed (4). Many factors associated with the prognosis and recurrence of HCC have now been reported. Vascular invasion of the portal vein and/or hepatic vein and tumor differentiation are important factors affecting survival and recurrence in HCC cases after a hepatectomy (5, 6). However, microvascular invasion and differentiation can only be detected by pathological examination just after a hepatectomy, and cannot be diagnosed preoperatively, this cannot be identified preoperatively either. Hence, the serum biomarkers alpha-fetoprotein (AFP) and protein induced by vitamin K absence-II (PIVKA-II) are used as prognostic markers (7, 8) and also as surrogate markers for microvascular invasion and tumor differentiation(9, 10). AFP is associated with grade differentiation (11), whereas PIVKA-II is related to vascular invasion (12, 13). However, these tumor markers have limited sensitivity and are less predictive than microvascular invasion (14, 15) which is the most potent determinant of recurrence and survival in HCC patients undergoing a hepatectomy(5). Therefore, new biomarkers that are more strongly